



LETTER

Harmonic Analysis of Worldwide Temperature Proxies for 2000 Years

Horst-Joachim Lüdecke^{1*} and Carl-Otto Weiss²¹HTW, University of Applied Sciences, Saarbrücken, Germany²CINVESTAV, Querétaro, Mexico; visiting from PTB Braunschweig, Mexico, Germany

Received: October 20, 2016

Revised: April 22, 2017

Accepted: April 27, 2017

Abstract: The Sun as climate driver is repeatedly discussed in the literature but proofs are often weak. In order to elucidate the solar influence, we have used a large number of temperature proxies worldwide to construct a global temperature mean G7 over the last 2000 years. The Fourier spectrum of G7 shows the strongest components as ~1000-, ~460-, and ~190 - year periods whereas other cycles of the individual proxies are considerably weaker. The G7 temperature extrema coincide with the Roman, medieval, and present optima as well as the well-known minimum of AD 1450 during the Little Ice Age. We have constructed by reverse Fourier transform a representation of G7 using only these three sine functions, which shows a remarkable Pearson correlation of 0.84 with the 31-year running average of G7. The three cycles are also found dominant in the production rates of the solar-induced cosmogenic nuclides ¹⁴C and ¹⁰Be, most strongly in the ~190 - year period being known as the De Vries/Suess cycle. By wavelet analysis, a new proof has been provided that at least the ~190-year climate cycle has a solar origin.

Keywords: Worldwide temperature proxies, Solar-climate cycles, Solar origin of the ~190 year climate cycle with new accuracy.

INTRODUCTION / OVERVIEW

Periodic or cyclic behaviour is so common in nature and physics that it gives the analysis technique of Fourier transform its outstanding importance. The reason for the abundance of cycles lies in the property of the transition from static to dynamic behaviour. This “modulational instability” occurs in space and time when the energy input into a dissipative system is increased beyond the range of static stability [1]. It leads overwhelmingly to a periodic state (rare exceptions exist, *e.g.* the Lorenz model, where the onset of dynamics is chaotic). The Sun and the Earth are classic dissipative systems with energy input. Cyclic dynamics is therefore to be expected. Cycles with periods ranging from several years to more than 100,000 years [2] have accordingly been observed, *e.g.* in paleoclimate studies.

The physical mechanism of climate cycles is mostly unknown and is not the main subject of this study. Autogeneous mechanisms and indirect solar forcing caused by the varying magnetic field of the Sun are discussed [3, 4, 5, 6]. Scafetta [7] provides evidence for the influence of planetary tides on the Sun, modulating the Sun's activity, cosmic ray flux and cloud formation by statistical correlation, and briefly discusses the assumed physical mechanism.

Concerning statistical correlation, Bond *et al.* [8] found an apparently solar-related 1500 year cycle. Liu *et al.* [9] found cycles of 1324, 800, 199, 110 years from tree rings in the Tibetan plateau. Kern *et al.* [10] reported on a late Miocene lake system indicating periods of 80, 120, 208, 500, 1000, and 1500 years. Zhao and Feng [11] found periods of 208, 521, and ~1000 years from Antarctic ice cores. Knudsen *et al.* [12, 13] observed correlation of the ~200 year De Vries/Suess cycle in spectrograms of solar activity with that of temperature variations in caves of China, Turkey, and the USA. Steinhilber and Beer [14] have investigated the solar activity of the last 10,000 years, finding strong indications of the De Vries/Suess cycle, and have predicted on these grounds a future temperature scenario. Babich *et al.* [15] have found periods of ~1000, ~500 to ~350, and ~200 years in paleoreconstruction of the last 2000 years,

* Address correspondence to this author at the HTW, University of Applied Sciences, Saarbrücken, Germany, Tel: 0049-6221-781052; E-mail: moluedecke@t-online.de

predicting a strongly pronounced cooling until AD 2500. In this context, we need to mention Schlesinger and Ramankutty [16], Gervais [17], De Vries [18], Suess [19], Steinhilber *et al.* [20, 21], Breitenmoser *et al.* [22], Cliver *et al.* [23], Raspopov *et al.* [24], Novello *et al.* [25], Wagner *et al.* [26], Lüdecke *et al.* [27, 28], Friis-Christensen and Lassen [29], Van Geel *et al.* [30], Braun *et al.* [31], Lohmann and Schöne [32], Czymzik *et al.* [33], Adolphi *et al.* [34], Wirth *et al.* [35], Lockwood [36], Fleitmann *et al.* [37], Svensmark [38], Svensmark *et al.* [6], Marsh and Svensmark [39], Enghoff [40], Gray *et al.* [41], Haigh [42, 43], Ineson *et al.* [44], Seidenglanz *et al.* [45], Kodera [46], Meehl *et al.* [47], and Leal-Silva and Herrera [48]. Lüning [49] provides an extensive compilation of pertinent references.

All climate-cycle investigations mentioned relate to local climate. In contrast to these, in the present work, we have investigated dominant cycles in worldwide temperature proxy data of the last 2000 years complemented by instrumental temperature measurements of global temperatures provided by HADCRUT4 [50], from AD 1850 onwards, and by RSS satellite data [51], from AD 1979 onwards.

Records of the cosmic isotopes ^{14}C and ^{10}Be found in tree rings and ice cores confirm that the magnetic field of the Sun had varied over distinct cycles in the past [14, 21]. We have elucidated the solar origin of the most pronounced climate cycles of ~ 1000 , ~ 460 , and ~ 190 year periods in our data. In particular, by wavelet analysis, we have confirmed the solar origin of the most prominent ~ 190 year cycle over 10,000 years with new accuracy.

The Data

We used paleotemperature reconstructions and instrumental temperature records for the construction of a global temperature record from AD 1 to AD 2015. For sufficient resolution of the Fourier analysis and to avoid possible distortions by interpolations, temperature reconstructions of 1-year time resolution are desirable. Unfortunately, these conditions are not generally given. As suitable records, we selected the instrumental global HADCRUT4 data [50] from 1850 to 2015 AD, the global RSS satellite temperature data [51] from 1979 to 2015 AD, and the following six paleotemperature reconstructions - their individual sites shown in Fig. (1).

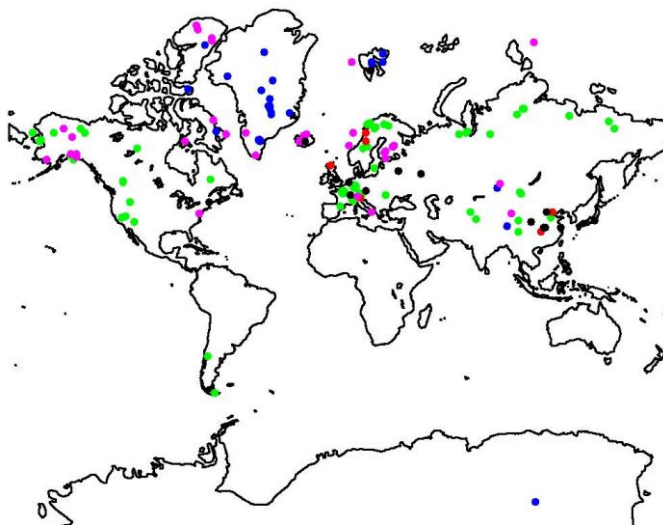


Fig. (1). (Color online) Locations of the proxy-temperature records used. Green color indicates tree-rings, blue ice-cores, red speleothems, magenta sediments, and black others.

1. (Chr) Christiansen and Ljungqvist [52]: stack of different temperature proxies [$^{\circ}\text{C}$], extracted from 91 single records, $\sim 30\%$ of them covering the total period, 0 to 1973 AD, 1 year time resolution, northern hemisphere.
2. (Bün) Büntgen *et al.* [53]: tree-rings, extracted from over thousand ring width series of central Europe, temperature anomaly [$^{\circ}\text{C}$], -499 to 2003 BC/AD, 1 year time resolution.
3. (McK) McKay and Kaufman [54]: stack of different temperature proxies [$^{\circ}\text{C}$], extracted from 59 single records, $\sim 20\%$ of them covering the whole period, 1 to 2000 AD, 1 year time resolution, Arctic 60° - 90° N.
4. (Vill-N) Villalba *et al.* [55]: tree-rings, temperature [$^{\circ}\text{C}$], 1640 to 1987 AD, 1 year time resolution, Patagonia-North $\sim 37^{\circ}$ S and (Vill-S): tree-rings, temperature [$^{\circ}\text{C}$], 1640 to 1993 AD, 1 year time resolution, Patagonia-South $\sim 55^{\circ}$ S.

5. (Pet) Petit *et al.* [2]: temperature anomaly [$^{\circ}\text{C}$] from δD of ice-cores, -420,000 to ~1950 BC/AD, 17 to 50 years time resolution, Antarctica.

All used records are temperature reconstructions. Thus no further data aggregation or formatting procedures were necessary. We constructed from the individual temperature reconstructions a global mean G7 as follows: Each reconstruction was normalized to an anomaly around the year 1950, thereby allowing for different mean temperatures at different latitudes. The satellite data beginning in 1979 were adjusted to the 1979 HADCRUT4 data.

Years before AD 1 in the reconstructions were omitted. For Bün, HADCRUT4 and Pet respectively the most recent years which show unusual deviations from the remaining reconstructions were also omitted. Next, for every year from AD 1 to AD 2015 the mean of these reconstructions which covered this particular year yields the pertinent temperature of G7. After that, G7, covering AD 1 to 2015, was again adjusted to an anomaly around its mean. Table 1 gives an overview of the data. The left panels of Fig. (2) show all reconstructions and G7 for the times specified in column “RL” of Table (1) (HADCRUT4 and RSS are not shown). G7 in more detail is depicted in the upper panel of Fig. (3) in grey and its 31-year running mean in blue color.

Table 1. Data details. All records are proxy-temperatures [$^{\circ}\text{C}$], except for Stei as the common production rate PC of the cosmogenic nuclides ^{14}C and ^{10}Be . BC/AD: length of the original record; RL: record length applied for constructing G7; Res.: Time resolution.

Record	BC/AD	RL	Res. [yr]	Location
Chr	0 - 1973	1 to 1973	1	NH
Bün	-499 to 2003	1 to 1990	1	Central Europe
McK	1 to 2000	1 to 2000	1	Arctic
Vill-N	1640 to 1987	1640 to 1987	1	Patagonia (N)
Vill-S	1640 to 1993	1640 to 1993	1	Patagonia (S)
Pet	-420,000 to ~2000	1 to 1950	17 to 50	Antarctica
HAD	1850 to 2015	1850 to 1979	1	global
RSS	1979 to 2015	1979 to 2015	1	global
G7	1 to 2015	1 to 2015	1	global
Stei	-7318 to 1988	/	22	global

For a comparison of global temperatures with the activity of the Sun, the cosmic-ray nuclides ^{14}C and ^{10}Be are an appropriate measure [56, 57, 20, 58, 21, 14]. We used a record of the common production rate of these nuclides that extends back to ~9500 years BP, here abbreviated as Stei [21] and evaluated from tree-rings and ice-cores. The characteristics of Stei are given in Table 1, its variation in time is shown in last row, column 2 of Fig. (2).

SPECTRAL ANALYSIS

For the discrete Fourier transformation, the individual reconstructions, converted to anomalies around the mean, were padded with 25,000 zeros to yield interpolation of the spectra. The false-alarm levels for the spectra were generated by Monte Carlo simulation, in each case with 10,000 random time series of identical length, anomaly around the mean, Hurst exponent and zero padding as the pertinent record. The Hurst exponents were obtained by detrended fluctuation analysis [59]. For the reconstructions Stei [21] and Pet [2], which are unevenly spaced and have time steps larger than 1 year, we first applied the method of Lomb [60] and Scargle [61]. Since this method yields the same results as the Fourier analysis of the records interpolated to one year steps, the Fourier analyses and the following wavelet analyses were carried out with the interpolated records. The right panels of Fig. (2) show the results of the spectral analyses.

For the longest records Pet [2] and Stei [21] wavelet analyses were applied and are shown in the two upper panels of Fig. (4). Wavelets give insight into the link of solar activity with Earth temperatures as described in the section “Sun's activity and climate”.

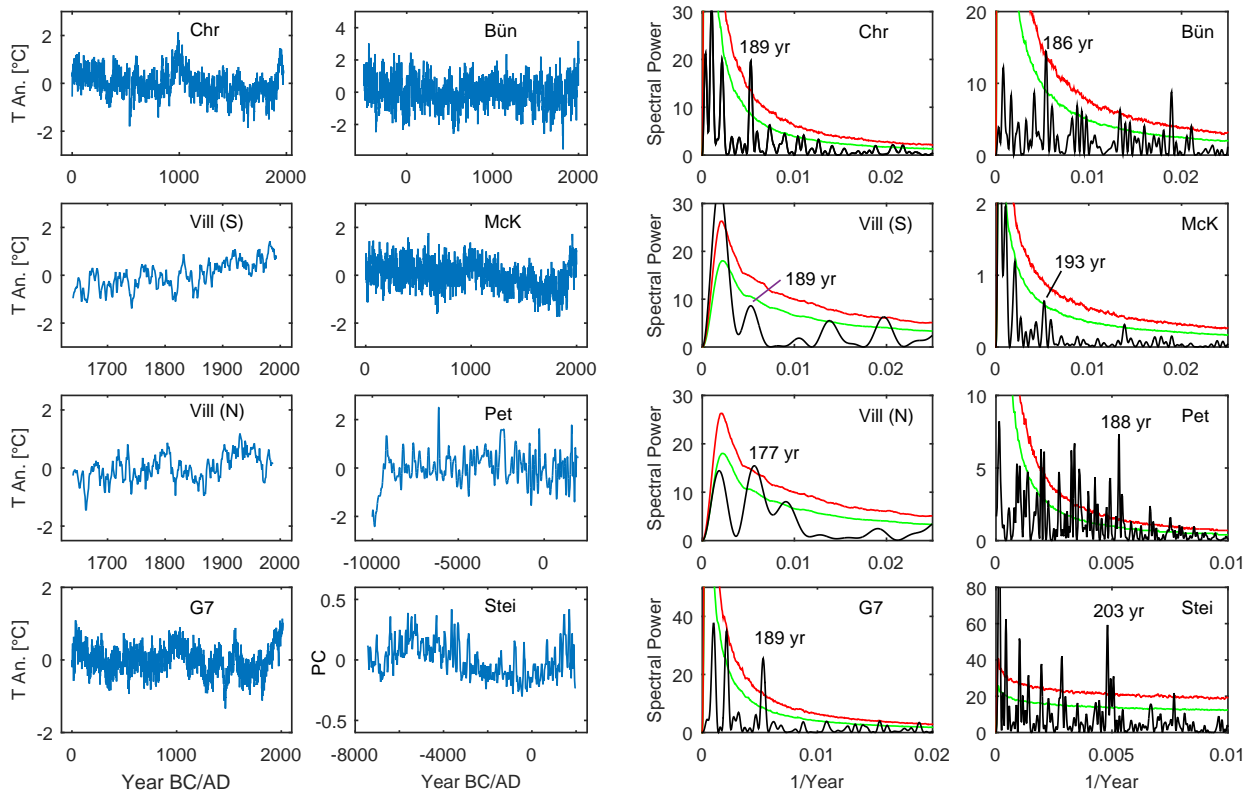


Fig. (2). (Color online) Left panels: Temperature records [°C] as anomalies around the mean, of Chr, Bün, McK, Vill-N, Vill-S, Pet, and the composite global record G7. The record of common production rate PC of the cosmogenic nuclides ¹⁴C and ¹⁰Be, Stei, is depicted in panel row 4, column 2. Right panels: Pertinent Fourier spectra with false-alarm lines of 95% (green) and 99% (red). The period of the strongest peak (generally ~190 year) is given.

RESULTS

Table 2 gives the periods corresponding to the strongest peaks of the spectra shown on the right hand side of Fig. (2).

Table 2. Strongest spectral peaks for the records Chr, Bün, McK, Vill-N, Vill-S, Pet, G7, and Stei for periods > 700 years, from 700 to 300 years, from 300 to 100 years, and < 100 years.

Record	> 700 years	700 to 300 years	300 to 100 years	< 100 years
Chr	998	467	189	48
Bün	1250	608	186	53
McK	964	491	193	72
Vill-N	/	/	177	/
Vill-S	/	/	189	51
Pet	948	499	188	/
G7	1003	463	188	65
Stei	991	508	203	/

There are substantial variations in the frequencies of obviously pertinent peaks in different records. Even for the same proxy (tree-rings) and sites apart by 2000 km, the ~190 - year period peaks of Vill-N and Vill-S differ by 12 years in period. Because we found no explanation for such differences in the literature we think that data noise is most likely the main cause of the deviations. As an attempt to test this assumption, we shortened the Bün record (total length 2503 years) in several steps to a minimum length of 1600 years. In the Fourier analyses of the shortened records we found values from 1250 to 1047 for the ~1000 - year period, from 608 to 408 for the ~460 - year period, and from 186 to 181 for the ~190 - year period. The averaging of a large number of data as used here can be expected to minimize the impact of such data inaccuracy.

The spectrum of the composite global record G7 has - much more distinctly than the individual records, likely due

to the averaging - the strongest peaks for the periods of 1003, 463, and 188 years. In particular, in the low frequency region practically no other peaks are visible. For the inverse Fourier transformation we used the mentioned longest three periods to obtain a representation of G7 with only three sine functions. These three cycles are already known from previous studies as cited in the section “Introduction/Overview”. This insures that the selected cycles are not artifacts of the Fourier transformation.

The upper panel of Fig. (3) shows the original G7 (grey), the 31-year running mean of G7 (blue) corresponding to the definition of “climate”, and the sine representation of G7 (green). Tentatively, we also constructed the representation with four sines including the ~60-year period (red).

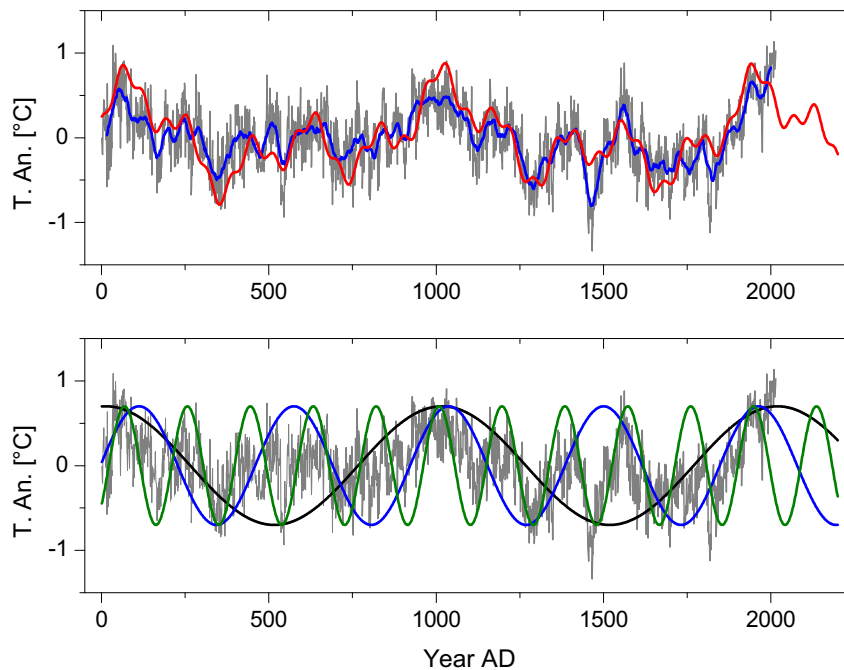


Fig. (3). (Color online) Upper panel: Global record G7 (grey), running 31-year average of G7 (blue), sine representation of G7 with three sine functions of the periods 1003, 463, and 188 years (green), with four sine functions including the period ~60 years (red), continued to AD 2200. The parameters of the sine functions are given in Table 3. The Pearson correlation between the 31 year running average of G7 and the three-sine representation (green) is 0.84, for the four-sine representation (red) 0.85. Lower panel: G7 (grey) together with the sine functions of 1003, 463, and 188 - year periods continued until AD 2200 (equal sine amplitudes for clarity).

The Pearson correlation of G7 and the three-sine representation is 0.65, while that with the 31-year running mean of G7 is remarkable 0.84. A four-sine representation which includes the ~60-year cycle improves this correlation only to 0.85. The ~60-year cycle is, however, important for shorter time studies. *e.g.* Gervais [17] shows that the ~60-year cycle explains the temperature plateau observed since the end of the 20th century.

The sine representation is continued in Fig. (3) until AD 2200 for future climate trends. It shows a drop from the present maximum to AD ~2050, a slight rise until AD ~2130 and a second drop to AD 2200. Babich *et al.* [15] come to similar conclusions.

The lower panel of Fig. (3) shows G7 (grey) together with the three sines of 1003, 463, and 188 - year periods of the representation (sine of ~60 years not shown). We emphasize that all three sines have maxima near AD 0, 1000, and 2000. (Table 3) cites the parameters of the sine representation.

Table 3. Representation of G7 by sine functions $S = A \cdot \sin(2\pi f \cdot (yr - 1) + \phi)$, f - frequency, p - period, A - amplitude (amplitudes multiplied with a common arbitrary factor for clarity of Fig. 3, ϕ - phase in radians).

f [1/yr]	$p = 1/f$ [yr]	A	ϕ
0.0009973	1002.7	0.3178	1.557
0.0021609	462.8	0.2840	0.097

(Table 5) contd....

f [1/yr]	p = 1/f [yr]	A	φ
0.0053191	188.0	0.2527	5.599
0.0154588	64.7	0.0899	1.990

Sun's Activity and Climate

Table (2) demonstrates that Stei [21] as the record mirroring the Sun's activity shows the same periods of ~1000, ~500, and ~200 years as found for the temperature record G7, suggesting the Sun as the main climate driver. This hypothesis is often emphasized in the literature (see references under "Introduction/Overview"). However, comparable periods alone would not be sufficient for excluding autogenous climate mechanisms.

To get more insight on a solar link with climate cycles we compared by wavelet analysis the temperatures of Pet [2] with the production rate of the cosmogenic nuclides ¹⁴C and ¹⁰Be of Stei [21] over 9000 years (see Table 1. and Fig. 2). The upper and middle panel of Fig. (4) show already by eyesight similarities in the power of the ~190 - year period over 9000 years, thus confirming earlier findings of Knudsen *et al.* [13].

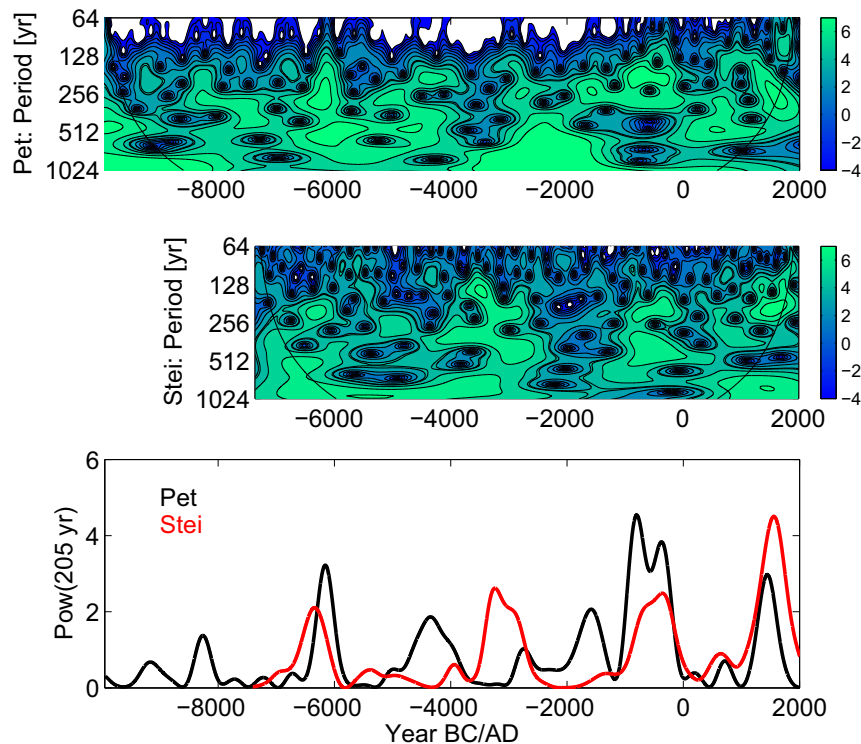


Fig. (4). (Color online) Upper panel: Wavelet spectrum of Antarctic temperatures Pet [2]. Middle panel: Wavelet spectrum of solar activity Stei [21]. Below the cone of influence, wavelet results are not significant. Lower panel: Spectral power for the period of ~190 years taken from the two wavelet spectra, powers in arbitrary units.

Next, we extracted from the wavelet spectra the power of the frequency component of the ~190 - year period both for Pet [2] and Stei [21]. Fig. (4) shows these power curves in the lower panel. There is good agreement from -7000 until -5000 BC and from -1000 BC until present. In between these times similarities still exist. This signature would seem strong enough to confirm the Sun as the main driver of at least the ~190 - year climate cycle. For the periods of ~1000 and ~460 years we could not find a similar power agreement between Stei and Pet.

DISCUSSION / CONCLUSION

The Fourier spectrum of a global temperature record G7, composed of high quality temperature proxies worldwide and recent instrumental data demonstrate the dominance of three climate cycles with ~1000 (Eddy cycle), ~460 (not named but frequently reported), and ~190 year periods (De Vries/Suess cycle). These three sines represent the 31-year

running mean of G7 with the remarkable Pearson correlation of 0.84 indicating their importance for climate.

G7, and likewise the sine representations have maxima of comparable size at AD 0, 1000, and 2000. We note that the temperature increase of the late 19th and 20th century is represented by the harmonic temperature representation, and thus is of pure multiperiodic nature. It can be expected that the periodicity of G7, lasting 2000 years so far, will persist also for the foreseeable future. It predicts a temperature drop from present to AD 2050, a slight rise from 2050 to 2130, and a further drop from AD 2130 to 2200 (see Fig. 3), upper panel, green and red curves).

As a main result of our study, the construction of a global record G7 from numerous temperature proxies reduces noise and thus allows the isolation of these global cycles. The dominance of the significant frequency components in the G7 spectrum, as opposed to the strength of other components in the spectra of the individual proxy records supports this view.

We provide a new confirmation for the link between solar activity and climate cycles by wavelet analysis showing a remarkably good agreement of the power of the ~190 - year period for temperatures and solar activity over 9000 years (see Fig. 4 lower panel). As (Fig. 2 and Table 2) show, the periods of ~1000 and ~460 years are also apparently common in records of temperatures and cosmogenic nuclides.

CONFLICT OF INTEREST

The authors declare no conflict of interest, financial or otherwise.

ACKNOWLEDGEMENTS

We express our thanks to the referees for valuable comments.

REFERENCES

- [1] Zakharov VE, Ostrovsky LA. Modulation instability: The beginning. *Physica D* 2009; 238: 540-8. [<http://dx.doi.org/10.1016/j.physd.2008.12.002>]
- [2] Petit JR, Jouzel J, Raynaud D, *et al.* Climate and atmospheric history of the past 420,000 years from the Vostok ice core, Antarctica. *Nature* 1999; 399: 429-36. Data available at <ftp://ftp.ncdc.noaa.gov/pub/data/paleo/icecore/antarctica/vostok/deutnat.txt> 2017. Last access: April 2017
- [3] Mazzarella A. The 60-year solar modulation of global air temperature: The Earth's rotation and atmospheric circulation connection. *Theor Appl Climatol* 2007; 88: 193-9. [<http://dx.doi.org/10.1007/s00704-005-0219-z>]
- [4] Mazzarella A. Solar Forcing of Changes in Atmospheric Circulation, Earth's Rotation and Climate. *Open Atmos Sci J* 2008; 2: 181-4. [<http://dx.doi.org/10.2174/1874282300802010181>]
- [5] Mazzarella A. Sun-climate linkage now confirmed. *Energy Environ* 2009; 20(1): 123-30. [<http://dx.doi.org/10.1260/095830509787689150>]
- [6] Svensmark H, Bondo T, Svensmark J. Cosmic ray decreases affect atmospheric aerosols and clouds. *Geophys Res Lett* 2009; 36(15). [<http://dx.doi.org/10.1029/2009GL038429>]
- [7] Scafetta N. Multi-scale harmonic model for solar and climate cyclical variation throughout the Holocene based on Jupiter-Saturn tidal frequencies plus the 11-year solar dynamo cycle. *J Atmos Sol Terr Phys* 2012; 80: 296-311. [<http://dx.doi.org/10.1016/j.jastp.2012.02.016>]
- [8] Bond G, Kromer B, Beer J, *et al.* Persistent solar influence on North Atlantic climate during the Holocene. *Science* 2001; 294(5549): 2130-6. [<http://dx.doi.org/10.1126/science.1065680>] [PMID: 11739949]
- [9] Liu Y, Cai Q, Song H, An Z, Linderholm HW. Amplitudes, rates, periodicities and causes of temperature variations in the past 2485 years and future trends over the central-eastern Tibetan Plateau. *Chin Sci Bull* 2011; 56: 2986-94. [<http://dx.doi.org/10.1007/s11434-011-4713-7>]
- [10] Kern AK, Harzhauser M, Piller WE, Mandic O, Soliman A. Strong evidence for the influence of solar cycles on a Late Miocene lake system revealed by biotic and abiotic proxies. *Palaeogeogr Palaeoclimatol Palaeoecol* 2012; 329-330(5): 124-36. [<http://dx.doi.org/10.1016/j.palaeo.2012.02.023>] [PMID: 23564975]
- [11] Zhao XH, Feng XS. Correlation between solar activity and the local temperature of Antarctica during the past 11,000 years. *J Atmos Sol Terr Phys* 2014; 122: 26-33. [<http://dx.doi.org/10.1016/j.jastp.2014.11.004>]
- [12] Knudsen MF, Riisager P, Jacobsen BH, Muscheler R, Snowball I, Seidenkrantz M-S. Taking the pulse of the Sun during the Holocene by joint analysis of ¹⁴C and ¹⁰Be. *Geophys Res Lett* 2009; 36(16). [<http://dx.doi.org/10.1029/2009GL039439>]
- [13] Knudsen MF, Jacobsen BH, Riisager P, Olsen J, Seidenkrantz M-S. Evidence of Suess solar-cycle bursts in subtropical Holocene speleothem

- $\delta^{18}\text{O}$ records. Holocene 2011; 22: 597-602.
[<http://dx.doi.org/10.1177/0959683611427331>]
- [14] Steinhilber F, Beer J. Prediction of solar activity for the next 500 years. *J Geophys Res-Space* 2013; 118: 1861-7.
[<http://dx.doi.org/10.1002/jgra.50210>]
- [15] Babich VV, Darin AV, Kalugin IA, Snolyaninova LG. Climate prediction for the extratropical northern hemisphere for the next 500 years based on periodic natural processes. *Russ Meteorol Hydrol* 2016; 41(9): 593-600.
[<http://dx.doi.org/10.3103/S1068373916090016>]
- [16] Schlesinger ME, Ramankutty N. An oscillation in the global climate system of period 65-70 years. *Nature* 1994; 367: 723-6.
[<http://dx.doi.org/10.1038/367723a0>]
- [17] Gervais F. Anthropogenic CO₂ warming challenged by 60-year cycle. *Earth Sci Rev* 2016; 155: 129-35.
[<http://dx.doi.org/10.1016/j.earscirev.2016.02.005>]
- [18] De Vries H. Variation in concentration of radiocarbon with time and location on Earth. *Koninkl Ned Akad Wetenschappen Proc* 1958; B61: 94-102.
- [19] Suess HE. The radiocarbon record in tree rings of the last 8000 years. *Radiocarbon* 1980; 22(2): 200-9.
[<http://dx.doi.org/10.1017/S0033822200009462>]
- [20] Steinhilber F, Abreu JA, Beer J. Solar modulation during the Holocene. *Astrophys Space Sci Trans* 2008; 4: 1-6.
[<http://dx.doi.org/10.5194/astra-4-1-2008>]
- [21] Steinhilber F, Abreu JA, Beer J, *et al.* 9,400 years of cosmic radiation and solar activity from ice cores and tree rings. *P Natl Acad Sci USA* 2012; 109: 5967-71. Data available at: ftp://ftp.ncdc.noaa.gov/pub/data/paleo/climate_forcing/solar_variability/steinhilber2012.txt (last access: April 2017).
- [22] Breitenmoser P, Beer J, Brönnimann S, Frank D, Steinhilber F, Wanner H. Solar and volcanic fingerprints in tree-ring chronologies over the past 2000 years. *Palaeogeogr Palaeoclimatol Palaeoecol* 2012; 313-314: 127-39.
[<http://dx.doi.org/10.1016/j.palaeo.2011.10.014>]
- [23] Cliver EW, Boriakoff V, Feynman J. Solar variability and climate change: Geomagnetic aa index and global surface temperature. *Geophys Res Lett* 1998; 25(7): 1035-8.
[<http://dx.doi.org/10.1029/98GL00499>]
- [24] Raspopov OM, Dergachev VR, Esper J, *et al.* The influence of the de Vries (~200-year) solar cycle on climate variations: Results from the Central Asian Mountains and their global link. *Palaeogeogr Palaeoclimatol Palaeoecol* 2008; 259: 6-16.
[<http://dx.doi.org/10.1016/j.palaeo.2006.12.017>]
- [25] Novello VF, Cruz FW, Karmann I, *et al.* Multidecadal climate variability in Brazil's Nordeste during the last 3000 years based on speleothem isotope records. *Geophys Res Lett* 2012; 39(23).
[<http://dx.doi.org/10.1029/2012GL053936>]
- [26] Wagner G, Beer J, Masarik J, *et al.* Presence of the solar De Vries cycle (~205 years) during the last ice age. *Geophys Res Lett* 2001; 28(2): 303-6.
[<http://dx.doi.org/10.1029/2000GL006116>]
- [27] Lüdecke H-J, Hempelmann A, Weiss CO. Multi-periodic climate dynamics: Spectral analysis of long-term instrumental and proxy temperature records. *Clim Past* 2013; 9: 447-52.
[<http://dx.doi.org/10.5194/cp-9-447-2013>]
- [28] Lüdecke H-J, Hempelmann A, Weiss CO. Paleoclimate forcing by the solar de Vries / Suess cycle. *Clim Past Discuss* 2015; 11: 279-305.
[<http://dx.doi.org/10.5194/cpd-11-279-2015>]
- [29] Friis-Christensen E, Lassen K. Length of the solar cycle: An indicator of solar activity closely associated with climate. *Science* 1991; 254(5032): 698-700.
[<http://dx.doi.org/10.1126/science.254.5032.698>] [PMID: 17774798]
- [30] Van Geel B, van der Plicht J, Renssen H. Major $\Delta^{14}\text{C}$ excursions during the late glacial and early Holocene: Changes in ocean ventilation or solar forcing of climate change? *Quat Int* 2003; 105: 71-6.
[[http://dx.doi.org/10.1016/S1040-6182\(02\)00152-0](http://dx.doi.org/10.1016/S1040-6182(02)00152-0)]
- [31] Braun H, Christl M, Rahmstorf S, *et al.* Possible solar origin of the 1,470-year glacial climate cycle demonstrated in a coupled model. *Nature* 2005; 438(7065): 208-11.
[<http://dx.doi.org/10.1038/nature04121>] [PMID: 16281042]
- [32] Lohmann G, Schöne BR. Climate signatures on decadal to interdecadal time scales as obtained from mollusk shells (*Arctica islandica*) from Iceland. *Palaeogeogr Palaeoclimatol Palaeoecol* 2013; 373: 152-62.
[<http://dx.doi.org/10.1016/j.palaeo.2012.08.006>]
- [33] Czymzik M, Muscheler R, Brauer A. Solar modulation of flood frequency in central Europe during spring and summer on interannual to multi-centennial timescales. *Clim Past* 2016; 12: 799-805.
[<http://dx.doi.org/10.5194/cp-12-799-2016>]
- [34] Adolphi F, Muscheler R, Svensson A, *et al.* Persistent link between solar activity and Greenland climate during the Last Glacial Maximum. *Nat Geosci* 2014; 7: 662-6.

- [http://dx.doi.org/10.1038/ngeo2225]
- [35] Wirth SB, Glur L, Gilli A, Anselmetti FS. Holocene flood frequency across the Central Alps - solar forcing and evidence for variations in North Atlantic atmospheric circulation. *Quat Sci Rev* 2013; 80: 112-28.
[http://dx.doi.org/10.1016/j.quascirev.2013.09.002]
- [36] Lockwood M. Solar influence on global and regional climates. *Surv Geophys* 2012; 33: 503-34.
[http://dx.doi.org/10.1007/s10712-012-9181-3]
- [37] Fleitmann D, Burns SJ, Mudelsee M, *et al.* Holocene forcing of the Indian monsoon recorded in a stalagmite from southern Oman. *Science* 2003; 300(5626): 1737-9.
[http://dx.doi.org/10.1126/science.1083130] [PMID: 12805545]
- [38] Svensmark H. Influence of cosmic rays on Earth's climate. *Phys Rev Lett* 1998; 81(22): 5027-30.
[http://dx.doi.org/10.1103/PhysRevLett.81.5027]
- [39] Marsh ND, Svensmark H. Low cloud properties influenced by cosmic rays. *Phys Rev Lett* 2000; 85(23): 5004-7.
[http://dx.doi.org/10.1103/PhysRevLett.85.5004] [PMID: 11102172]
- [40] Enghoff MB, Pedersen JO, Uggerhoj UI, Paling SM. Aerosol nucleation induced by a high energy particle beam. *Geophys Res Lett* 2011; 38(9).
[http://dx.doi.org/10.1029/2011GL047036]
- [41] Gray LJ, Beer J, Geller M, *et al.* Solar influences on climate. *Rev Geophys* 2010; 48(4)
[http://dx.doi.org/10.1029/2009RG000282]
- [42] Haigh JD. The role of stratospheric ozone in modulating the solar radiative forcing of climate. *Nature* 1994; 370: 544-6.
[http://dx.doi.org/10.1038/370544a0]
- [43] Haigh JD. The impact of solar variability on climate. *Science* 1996; 272(5264): 981-4.
[http://dx.doi.org/10.1126/science.272.5264.981] [PMID: 8662582]
- [44] Ineson S, Scaife AA, Knight JR, *et al.* Solar forcing of winter climate variability in the Northern Hemisphere. *Nat Geosci* 2011; 4: 753-7.
[http://dx.doi.org/10.1038/ngeo1282]
- [45] Seidenglanz A, Prange M, Varma V, Schulz M. Ocean temperature response to idealized Gleissberg and de Vries solar cycles in a comprehensive climate model. *Geophys Res Lett* 2012; 39(22).
[http://dx.doi.org/10.1029/2012GL053624]
- [46] Kodera K. Solar cycle modulation of the North Atlantic Oscillation: Implication in the spatial structure of the NAO. *Geophys Res Lett* 2002; 29(8)
[http://dx.doi.org/10.1029/2001GL014557]
- [47] Meehl GA, Washington WM, Wigley TM, Arblaster JM, Dai A. Solar and greenhouse gas forcing and climate response in the twentieth century. *J Clim* 2002; 16: 426-44.
[http://dx.doi.org/10.1175/1520-0442(2003)016<0426:SAGGFA>2.0.CO;2]
- [48] Leal-Silva MC, Velasco Herrera VM. Solar forcing on the ice winter severity index in the western Baltic region. *J Atmos Sol Terr Phys* 2012; 89: 98-109.
[http://dx.doi.org/10.1016/j.jastp.2012.08.010]
- [49] Lüning S. Compilation of references of solar-climate cycles available at www.klimaargumente.de/#sonne 2014 (last access: April 2017), and chronos.qub.ac.uk/blaauw/cds.html 2017. (last access: April).
- [50] Climatic Research Unit, University of East Anglia. Data available at <https://crudata.uea.ac.uk/cru/data/temperature/> 2017. (last access: April)
- [51] Remote Sensing System (USA). Data available at <http://www.remss.com/measurements/upper-air-temperature> 2017. (last access: April).
- [52] Christiansen B, Ljungqvist FC. The extra-tropical Northern Hemisphere temperature in the last two millennia: reconstructions of low-frequency variability. *Clim Past* 2012; 8: 765-786. Data available at ftp://ftp.ncdc.noaa.gov/pub/data/paleo/contributions_by_author/christiansen2012/christiansen2012.txt 2017. (last access: April).
- [53] Büntgen U, Tegel W, Nicolussi K, *et al.* 2500 years of European climate variability and human susceptibility. *Science* 2011; 331: 578-582. Data available at <ftp://ftp.ncdc.noaa.gov/pub/data/paleo/treering/reconstructions/europe/buentgen2011europe.txt> 2017. (last access: April)
- [54] McKay NP, Kaufmann DS. An extended Arctic proxy temperature database for the past 2,000 years. *Sci Data* 2014; 1(140026). Data available at <http://ncdc.noaa.gov/paleo/study/16973> 2017. (last access: April).
- [55] Villalba R, Boninsegna JA, Masiokas M, *et al.* Large-Scale Temperature Changes Across the Southern Andes: 20th-Century Variations in the Context of the Past 400 Years. *Climatic Change* 2003; 59: 177-232. Data available at: <ftp://ftp.ncdc.noaa.gov/pub/data/paleo/treering/reconstructions/southamerica/patagonia-temperature.txt> 2017. (last access: April).
- [56] Stuiver M, Reimer PJ, Bard E, *et al.* INTCAL98 radiocarbon age calibration, 24,000-0 cal BP. *Radiocarbon* 1998; 40(3): 1041-83.
[http://dx.doi.org/10.1017/S0033822200019123]
- [57] Bard E, Raisbeck GM, Yiou F, Jouzel J. Solar modulation of cosmogenic nuclide production over the last millennium: comparison between ¹⁴C and ¹⁰Be records. *Earth Planet Sci Lett* 1997; 150: 453-62.
[http://dx.doi.org/10.1016/S0012-821X(97)00082-4]

- [58] Muschelers R, Beer J, Kubicki P, Synal H-A. Geomagnetic field intensity during the last 60,000 years based on ^{10}Be and ^{36}Cl from the Summit ice cores and ^{14}C . *Quat Sci Rev* 2005; 24: 1849-60.
[<http://dx.doi.org/10.1016/j.quascirev.2005.01.012>]
- [59] Kantelhardt JW, Koscielny-Bunde E, Rego HH, Havlin S, Bunde A. Detecting long-range correlations with detrended fluctuation analysis. *Physica A* 2001; 295: 441-54.
[[http://dx.doi.org/10.1016/S0378-4371\(01\)00144-3](http://dx.doi.org/10.1016/S0378-4371(01)00144-3)]
- [60] Lomb NR. Least-squares frequency analysis of unequally spaced data. *Astrophys Space Sci* 1967; 39(2): 447-62.
[<http://dx.doi.org/10.1007/BF00648343>]
- [61] Scargle JD. Studies in astronomical time series analysis. II - Statistical aspects of spectral analysis of unevenly spaced data. *Astrophys J* 1982; 263: 835-53.
[<http://dx.doi.org/10.1086/160554>]

© 2017 Lüdecke and Weiss.

This is an open access article distributed under the terms of the Creative Commons Attribution 4.0 International Public License (CC-BY 4.0), a copy of which is available at: <https://creativecommons.org/licenses/by/4.0/legalcode>. This license permits unrestricted use, distribution, and reproduction in any medium, provided the original author and source are credited.